# Technical Notes

*TECHNICAL NOTES are short manuscripts describing new developments or important results of a preliminary nature. These Notes cannot exceed 6 manuscript pages and 3 figures; a page of text may be substituted for a figure and vice versa. After informal review by the editors, they may be published within a few months of the date of receipt. Style requirements are the same as for regular contributions (see inside back cover).*

## Unsteady Streamlines near the Trailing Edge of NACA 0012 Airfoil at a Reynolds Number of 125,000

Xiao L. Liu,* Andrew Wo,† and Eugene E. Covert‡
*Universitat Karlsruhe, Karlsruhe, Federal Republic of Germany*

THE purpose of this Note is to present some new results on the unsteady streamlines near the trailing edge of a NACA 0012 airfoil with a chord of 508 mm. The unsteady flow is developed by a rotating ellipse located downstream and below the airfoil. This experimental arrangement has been described previously.[1-3] Note that those experiments were conducted in the Wright Brothers Wind Tunnel, while this experiment was conducted in the MIT Low Turbulence Wind Tunnel.[4] While this change is one of convenience, there is a difference in turbulence level. At a Reynolds number of 125,000, the turbulence level is 0.05% in the Low Turbulence Wind Tunnel and 0.8% in the Wright Brothers Wind Tunnel.

The analysis in Ref. 1 shows that the excitation of the flow by the rotating ellipse is a constant phase excitation for all practical purposes. The NACA 0012 airfoil was mounted between two end-plates that spanned the tunnel.[1] Figure 1 shows the positions at which the velocity was measured. The nearest position was 0.2% chord downstream of the trailing edge or about 0.8% of the trailing-edge height downstream.

For this experiment the Mach number is 0.09 and the reduced frequency based upon the half-chord ($k$) was 2.0. Clearly, the flow can be considered to be incompressible. Fletcher[5] measured the boundary-layer velocity profiles at 94% chord at this Reynolds number. At $k=2$, the mean displacement thickness there is of the order of 2.5 times the thickness of the trailing edge; the shape factor is about 1.5. The variation of the mean displacement thickness $\delta^*$ with $k$ was roughly independent of Reynolds number. Mean displacement thickness $\delta^*$ was approximately constant or at most increased slowly with $k$ for $k$ greater than about 1.5. Note that the Reynolds number was held constant at 125,000, 400,000, and 700,000 while $k$ varied. In this experiment the velocity was measured near the trailing edge with a two-color TSI 9100-7 Laser Doppler Anemometer that was calibrated against the speed of rotating gear teeth and found to be accurate to $\pm 0.18\%$.

The ellipse induces a nonuniform upwash over the chord, which can be characterized by the angle of attack at the trailing edge. The unsteady angle of attack is 9 deg ± 4.6 deg for this geometry. It was measured to ± 0.4 deg. The unsteady data was reduced by ensemble averaging. The output of the anemometer was recorded at constant phase referenced to rotation position of the ellipse that provided the unsteady excitation. At each phase the data was averaged for 150 cycles. This process was repeated nine independent times and then averaged. Although the chord Reynolds Number was low (125,000), the ensemble averaging removed random signals that might be due to turbulence in the flow or to other random noise. The distribution functions of the velocity are shown in Fig. 2. These histograms show the distribution of the number of counts $N$ (ordinate) at each speed $U$ (abcissa). If $N(U)$ is to represent a probability distribution, the area under the curve must be unity. Hence, a scale factor $f$ is needed to insure that that restraint is met. Variable $f$ is also shown on the figure. The double hump in the distribution function is interpreted as resulting from the interaction between the upper-surface separation surface and the separation surface from the lower-surface trailing edge and leads to a Karman vortex shedding in the wake. This interpretation follows that of Hathaway et al.[6] This double hump persists downstream of the last measuring point at one-fifth of the chord downstream from the trailing edge. The temporal mean was extracted from the ensemble averages by averaging over the period of the excitation.

The reduced data were the ratios of each velocity component in the unsteady flow to the freestream value at each phase

Measurement Location Points

| x/c | x-x$_{T.E.}$ (mm) | ΔY (mm) |
|---|---|---|
| 1.002 | 1.0 | 1.0 |
| 1.025 | 12.7 | 1.5 |
| 1.050 | 25.4 | 2.0 |
| 1.075 | 38.1 | 3.0 |
| 1.100 | 50.8 | 4.0 |
| 1.125 | 63.5 | 5.0 |
| 1.150 | 76.2 | 6.0 |
| 1.175 | 88.9 | 7.0 |
| 1.200 | 101.6 | 8.0 |

**Fig. 1 Location of velocity measuring points.**

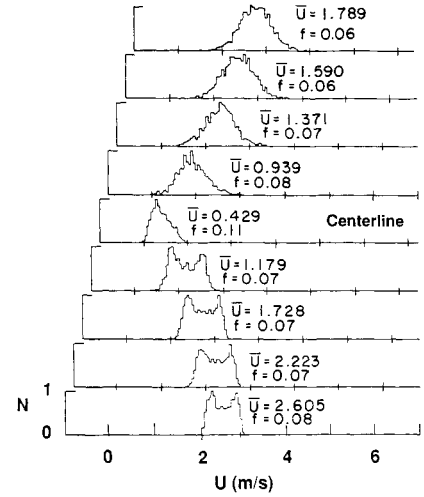


**Fig. 2 Transverse velocity probability distributions; $x/c=1.002$, centerline ($y=0$) is at $U=0.429$, $\alpha=0$ deg, $k=2$, $Re=125{,}000$.**

Received Oct. 25, 1988; revision received Feb. 25, 1989. 

*Research Associate
†Research Assistant, Department of Aeronautics and Astronautics.
‡Professor, Department Head, Department of Aeronautics and Astronautics. Fellow AIAA.

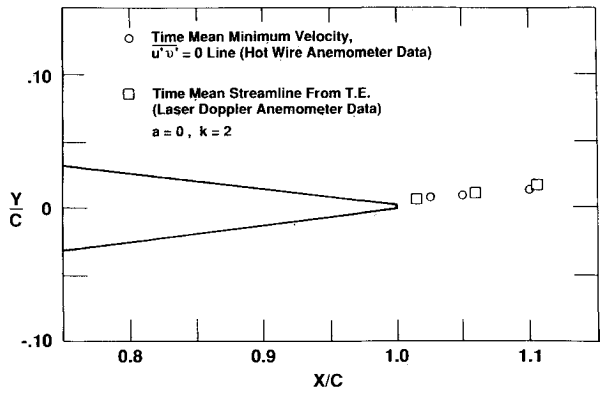


**Fig. 3 Comparison of mean zero streamline; $\alpha = 0$ deg, $k = 2$, $Re = 125{,}000$.**

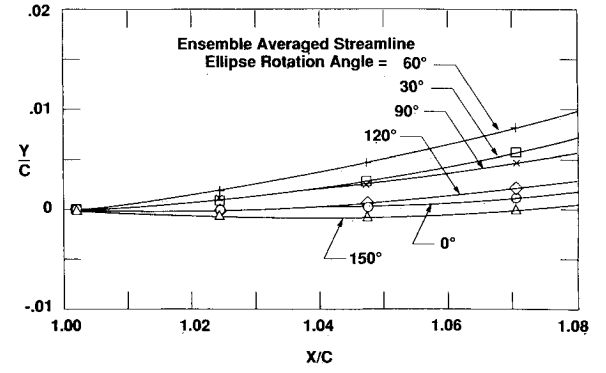


**Fig. 4 Ensemble-averaged streamline at different ellipse angles; $\alpha = 0$ deg, $k = 2$, $Re = 125{,}000$.**

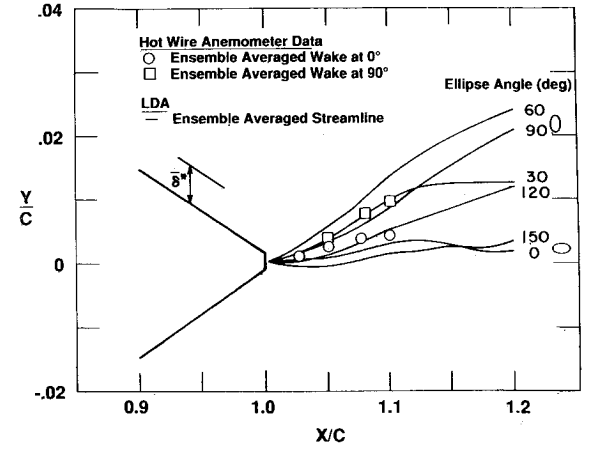


**Fig. 5 Ensemble-averaged streamline 5:1 vertical exaggeration (same conditions as Fig. 4).**

(point in time). The mean and ensemble-averaged streamlines were found by numerical path integration. Standard interpolation procedures were used to provide an estimate of the velocity distribution between measuring stations.

Figure 3 shows the mean wake streamline as the locus of both the minimum of the tangential velocity component and the locus where the Reynolds stress changes sign, as determined by a hot-wire anemometer and by integration of the laser anemometer data. These two loci seem to be coincident within our ability to measure them.

The ensemble-averaged streamline is shown in Fig. 4. The geometric scale is enlarged for clarity. Each curve corresponds to a rotation position or phase of the excitation. This same data is shown in Fig. 5 with a greater vertical magnification (5:1) along with the trailing-edge geometry. That figure also shows the time mean displacement thickness at 94% chord and the steady streamline for 0- and a 90-deg ellipse angles. The shed vorticity is increasing near zero ellipse angle. This tends to cause the streamline shape to fall below the mean streamline. The contrary is true at 90 deg when the shed vorticity tends to raise the streamline when compared to the steady flow distortion due to the ellipse. An interesting detail is that the streamline position remains within the triangle defined by the extension of the upper and lower surfaces, as discussed by Basu and Hancock[7] and Poling and Telionis.[8]

The latter present data that show smooth motion of streamlines near the trailing edge of an oscillating airfoil in an otherwise steady flow.

In our case where the working fluid is in motion and the airfoil is fixed, the motion of the streamlines also followed the motion of the fluid smoothly. Both these experiments have a constant phase excitation. It is also likely that the boundary layer in the Poling-Telionis experiment was laminar, while ours was either in late transition or turbulent. [Poling and Telionis reported strong curvature of the trailing-edge streamline when the excitation is due to convecting vortices past a fixed airfoil (c.f. their Fig. 11). In that experiment the airfoil was excited by a moving vortex field that contained traveling fluctuation of both longitudinal and transverse components. [The curvature in the streamline reported in Ref. 8 seems to occur when a traveling disturbance interacts with a fixed airfoil.] Thus, for a constant phase excitation, the streamline comes off the trailing edge smoothly when the airfoil is in motion in a fixed stream or when the stream is in motion and the airfoil is fixed, for either a laminar or transitional boundary layer.

## Acknowledgments

This research was sponsored in part by the Office of Naval Research Grant N0014-86-K-0513, Dr. S. G. Lekoudis, Project Monitor, and in part by a grant from the Grumman Aircraft and Engineering Company to the MIT Center for Aerodynamic Studies.

## References

[1]Lorber, P. F. and Covert, E. E., "Unsteady Airfoil Pressures Produced by Periodic Aerodynamic Interference," *AIAA Journal,* Vol. 20, Sept. 1982, pp. 1153-1159.

[2]Covert, E. E. and Lorber, P. F., "Unsteady Turbulent Boundary Layers in Adverse Pressure Gradients," *AIAA Journal,* Vol. 22, Jan. 1984, pp. 22-28.

[3]Covert, E. E., Lorber, P. F., and Vaczy, C. M., "Measurements of the Near Wake of an Airfoil in Unsteady Flow," AIAA Paper 83-0127, Jan. 1983.

[4]Mangus, J. F., "Measurement of Drag and Bursting Frequency Downstream of Tandem Spanwise Ribbons in a Turbulent Boundary Layer," SM Thesis in Aeronautics and Astronautics, MIT, 1984.

[5]Fletcher, M. J., "Reynolds Number Effects the Unsteady Aerodynamic Behavior of an NACA 0012 Airfoil," MIT, SM Thesis in Aeronautics and Astronautics, Sept. 1986.

[6]Hathaway, M. D., Gertz, J. B., Epstein, A. H., and Strazisar, A. J., "Rotor Wake Characteristics of a Transonic Axial-Flow Fan," *AIAA Journal,* Vol. 24, Nov. 1986, pp. 1802-1810.

[7]Basu, B. C. and Hancock, G. J., "The Unsteady Motion of a Two-Dimensional Airfoil in Incompressible Inviscid Flow," *Journal of Fluid Mechanics,* Vol. 87, Part 1, 1978, pp. 159-178.

[8]Poling, D. R. and Telionis, D. P., "The Response of Airfoils to Periodic Disturbances—The Unsteady Kutta Condition," *AIAA Journal,* Vol. 24, Feb. 1986, p. 193.